PROCEEDINGS OF SCIENCE

Diffractive dijets at HERA and EIC using GTMDs

Barbara Linek,[a,*] **Marta Łuszczak,**[b] **Wolfgang Schäfer**[c] **and Antoni Szczurek**[b,c]

[a] *Doctoral School of the University of Rzeszów, University of Rzeszów, st Rejtana 16C, 35-959 Rzeszów, Poland*

[b] *College of Natural Sciences, Institute of Physics, University of Rzeszów, st Rejtana 16C, 35-959 Rzeszów, Poland*

[c] *Institute of Nuclear Physics, Polish Academy of Sciences, ul. Radzikowskiego 152, PL-31-342 Kraków, Poland*

E-mail: barbarali@dokt.ur.edu.pl, mluszczak@ur.edu.pl, Wolfgang.Schafer@ifj.edu.pl, antoni.szczurek@ifj.edu.pl

We calculate differential distributions for diffractive dijets production in $ep \to e' p\ jet\ jet$ reaction using off diagonal unintegrated gluon distributions (GTMDs). Different models are used. We concentrate on the contribution of exclusive $q\bar{q}$ dijets.

The results of our calculations are compared to H1 and ZEUS data. In general, except of one GTMD, our results are below the HERA data. This is in contrast with recent results where the normalization was adjusted to some selected distributions and no agreement with other observables was checked. We conclude that the calculated cross sections are only a small part of the measured ones which probably also contain processes with pomeron remnant, reggeon exchange, etc.

We also present azimuthal correlations between the sum and the difference of dijet transverse momenta. The cuts on transverse momenta of jets generate azimuthal correlations which can be misinterpreted as due to so-called elliptic GTMD.

42nd International Conference on High Energy Physics (ICHEP2024)
18-24 July 2024
Prague, Czech Republic

*Speaker

https://pos.sissa.it/

PoS(ICHEP2024)506

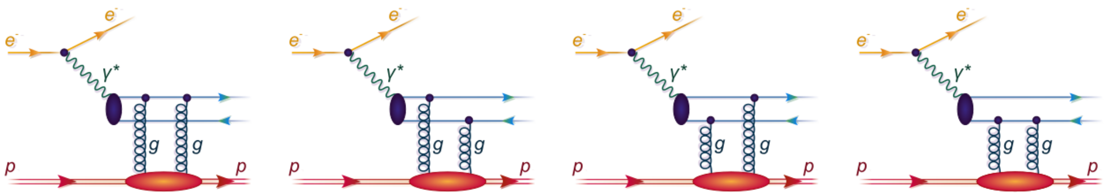

Figure 1: Four types of the diffractive production of dijets in electron-proton collisions.

1. Sketch of the formalism

This work focuses on exclusive, diffractive dijet production in the $ep \to ejjp$ reaction, where the final-state proton remains in its ground state, measured by the H1 [1] and ZEUS [2] collaborations. We use a formalism derived from the color dipole approach but the dipole amplitude information from impact parameter space is mapped to off-forward transverse momentum-dependent gluon distributions (GTMDs). For reviews linking this to the gluon Wigner function, see [3]. At large jet momenta, the forward diffractive amplitude directly probes the unintegrated gluon distribution of the target [4, 5]. While this approach is suited for the small-x limit, longitudinal momentum transfer and skewedness are handled in a collinear factorization framework using generalized parton distributions, as in [6]. This work includes also $q\bar{q}$ exchanges in the t-channel, relevant for smaller rapidity gaps.

In [7], we applied various GTMD models to the $pA \to c\bar{c}pA$ process, although no data is available yet due to the challenges of relevant measurements. Here, we apply the same formalism to H1 and ZEUS data, comparing different GTMD models with existing data.

Recent theoretical calculations on diffractive dijet production, using either the color dipole or GTMD approaches, include [8–13]. While some of these works focus on photoproduction or heavy quarks, our study has some overlap with [8], which uses the Golec-Biernat–Wüsthoff parametrization [14] for the dipole amplitude. For the corresponding gluon distribution, our results agree with the other. However, we also employ the GTMDs proposed and fitted in [12, 13] and our conclusions differ from these works.

To calculate the cross section for $ep \to ep\, q\bar{q}$ both, the transverse σ_T and longitudinal σ_L photon components have to be included:

$$\frac{d\sigma^{ep}}{dydQ^2d\xi} = \frac{\alpha_{em}}{\pi y Q^2}\Big[\Big(1-y+\frac{y^2}{2}\Big)\frac{d\sigma_T^{\gamma^* p}}{d\xi} + (1-y)\frac{d\sigma_L^{\gamma^* p}}{d\xi}\Big], \tag{1}$$

where $d\xi = dz d^2\vec{P}_\perp d^2\vec{\Delta}_\perp$, while the interferences between photon polarizations are neglected as they vanish when averaging over the angle between the electron scattering and hadronic planes.

For all four mechanisms from Fig.1, the $\gamma^* p \to q\bar{q}p$ cross sections for transverse and longitudinal photons are given by:

$$\begin{aligned}\frac{d\sigma_T^{\gamma^* p}}{dz d^2\vec{P}_\perp d^2\vec{\Delta}_\perp} &= 2N_c\alpha_{em}\sum_f e_f^2 \int d^2\vec{k}_\perp \int d^2\vec{k}_\perp{}' T(Y,\vec{k}_\perp,\vec{\Delta}_\perp) T(Y,\vec{k}_\perp{}',\vec{\Delta}_\perp) \\ &\times \left\{ \left(z^2+(1-z)^2\right)\left[\frac{(\vec{P}_\perp-\vec{k}_\perp)}{(\vec{P}_\perp-\vec{k}_\perp)^2+\epsilon^2} - \frac{\vec{P}_\perp}{P_\perp^2+\epsilon^2}\right]\cdot\left[\frac{(\vec{P}_\perp-\vec{k}_\perp{}')}{(\vec{P}_\perp-\vec{k}_\perp{}')^2+\epsilon^2} - \frac{\vec{P}_\perp}{P_\perp^2+\epsilon^2}\right]\right. \\ &+ \left. m_f^2\left[\frac{1}{(\vec{P}_\perp-\vec{k}_\perp)^2+\epsilon^2} - \frac{1}{P_\perp^2+\epsilon^2}\right]\cdot\left[\frac{1}{(\vec{P}_\perp-\vec{k}_\perp{}')^2+\epsilon^2} - \frac{1}{P_\perp^2+\epsilon^2}\right]\right\}, \end{aligned} \quad (2)$$

$$\begin{aligned}\frac{d\sigma_L^{\gamma^* p}}{dz d^2\vec{P}_\perp d^2\vec{\Delta}_\perp} &= 2N_c\alpha_{em}4Q^2z^2(1-z)^2 \times \sum_f e_f^2 \int d^2\vec{k}_\perp \int d^2\vec{k}_\perp{}' T(Y,\vec{k}_\perp,\vec{\Delta}_\perp) T(Y,\vec{k}_\perp{}',\vec{\Delta}_\perp) \\ &\times \left[\frac{1}{(\vec{P}_\perp-\vec{k}_\perp)^2+\epsilon^2} - \frac{1}{P_\perp^2+\epsilon^2}\right]\cdot\left[\frac{1}{(\vec{P}_\perp-\vec{k}_\perp{}')^2+\epsilon^2} - \frac{1}{P_\perp^2+\epsilon^2}\right], \end{aligned} \quad (3)$$

with $\epsilon^2 = z(1-z)Q^2 + m_f^2$ and the generalized transverse momentum distribution (GTMD) of gluons in the proton target expressed as a Fourier transform of the diffraction amplitude in momentum space (see [3, 9–11]):

$$T(Y,\vec{k}_\perp,\vec{\Delta}_\perp) = \int \frac{d^2\vec{b}_\perp}{(2\pi)^2}\frac{d^2\vec{r}_\perp}{(2\pi)^2} e^{-i\vec{\Delta}_\perp\cdot\vec{b}_\perp} e^{-i\vec{k}_\perp\cdot\vec{r}_\perp} N(Y,\vec{r}_\perp,\vec{b}_\perp)\, e^{-\varepsilon r_\perp^2}. \quad (4)$$

The used normalization is consistent with Ref. [11] and $\varepsilon = (0.5\,\mathrm{fm})^{-2}$ is used in the calculation. We also analyzed the correlations in azimuthal angle between the sum and difference of transverse moment of jets:

$$\cos\phi_{\vec{P}_\perp\vec{\Delta}_\perp} = \frac{\vec{P}_\perp\cdot\vec{\Delta}_\perp}{P_\perp\Delta_\perp}, \quad (5)$$

where

$$\vec{P}_\perp = \frac{1}{2}(\vec{p}_{\perp 1} - \vec{p}_{\perp 2}), \qquad \vec{\Delta}_\perp = \vec{p}_{\perp 1} + \vec{p}_{\perp 2}. \quad (6)$$

We consider six different models for generalized transverse momentum distributions (GTMDs). Two of these are parameterizations of off-forward gluon density matrices based on diagonal unintegrated gluon distributions: Golec-Biernat–Wüsthoff (GBW) model [14] and Moriggi-Paccini-Machado (MPM) model [15]. Both use a diffractive slope of $B = 4$ GeV^{-2}:

$$f\left(Y, \frac{\vec{\Delta}_\perp}{2}+\vec{k}_\perp, \frac{\vec{\Delta}_\perp}{2}-\vec{k}_\perp\right) = \frac{\alpha_s}{4\pi N_c}\frac{\mathcal{F}(x_{\mathbb{P}},\vec{k}_\perp,-\vec{k}_\perp)}{k_\perp^4}\exp\left[-\frac{1}{2}B\vec{\Delta}^2\right]. \quad (7)$$

The other four models are derived from the Fourier transform of the dipole amplitude described by equation (4).

We use also the bSat model of Kowalski and Teaney [16] (KT model), as well as three models based on the McLerran-Venugopalan (MV) approach [17]. These include the Iancu-Rezaeian model

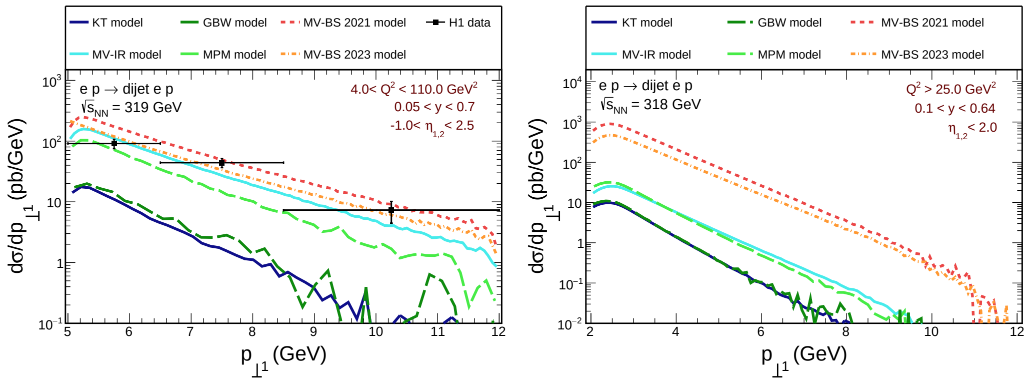

Figure 2: Distribution of the cross-section for the diffractive light dijet production in jet transverse momentum for H1(left) and ZEUS (right) kinematic for different GTMDs.

(MV-IR) [18], the Boer-Setyadi 2021 model (MV-BS 2021) [12], and the Boer-Setyadi 2023 model (MV-BS 2023) [13], which ware fitted to the H1 experimental data. In addition, we modified the MV-IR model using $\lambda = 0.277$:

$$T^{\rm mod}_{\rm MV-IR}(Y,\vec{k}_\perp,\vec{\Delta}_\perp) = T_{\rm MV-IR}(\vec{k}_\perp,\vec{\Delta}_\perp)\,e^{\lambda Y}, \qquad Y = \ln\left[\frac{0.01}{x_{\mathbb{P}}}\right]. \tag{8}$$

To adopt the MV-BS 2021 to the H1 data [1] we add according to [12] $\chi = 1.25$ in the expression:

$$N_0(r_\perp,b_\perp) = -\frac{1}{4}r_\perp^2\chi Q_s^2(b_\perp)\ln\left[\frac{1}{r_\perp^2\lambda^2}+e\right], \quad Q_s^2(b_\perp) = \frac{4\pi\alpha_s C_F}{N_c}\exp\left[\frac{-b_\perp^2}{2R_p^2}\right]. \tag{9}$$

For MV-BS 2023 the $\chi(x_{Bj}) = \bar{\chi}\left(\frac{x_0}{x_{Bj}}\right)^{\lambda_\chi}$, where $\bar{\chi} = 1.5$, $x_0 = 0.0001$ and $\lambda_\chi = 0.29$ according to [13] is used.

2. Results

Our calculations were divided into two areas according to the kinematics of the H1 and ZEUS collaborations. We first show the distributions in the transverse momentum of the jet seen in Fig. 2. The MV-BS 2021 and MV-BS 2023 give similar results to the MV-IR and MPM models and describe the data quite well, while the KT and GBW distributions are lower by an order of magnitude than the experimental data. Both the MV-BS results for the ZEUS kinematics differ by almost two orders of magnitude from other GTMDs however, the shapes of all distributions are comparable. We also generated distributions in $x_{\mathbb{P}}$ and β shown in Figs 3, where the differences between all models are visible. In the case of the dependence on $x_{\mathbb{P}}$, overestimated data by all GTMD models except KT and GBW are visible. This may be related to the fact that correct description of all experimental data is possible considering not only the dipole approach but rather the contribution of $q\bar{q}$ described by secondary Reggeons, e.g. in Ref. [19].

The distributions in β also show inconsistencies with the data of the MV-BS models that were fitted to the H1 experiment. In contrast, the other models give results too low for small β, however, this area should be described by the $q\bar{q}g$ three-parton contribution. In Fig. 4 we show the

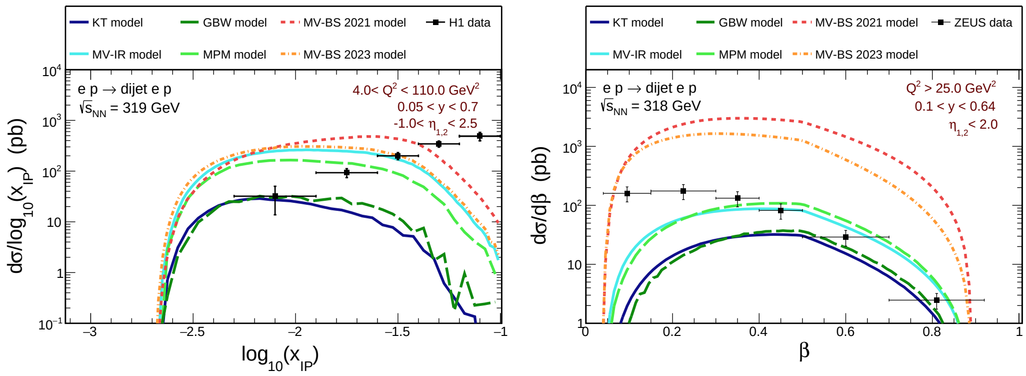

Figure 3: Distribution of the cross-section for the diffractive light dijet production in $x_{\mathbb{P}}$ and β for H1 and ZEUS kinematic for different GTMDs.

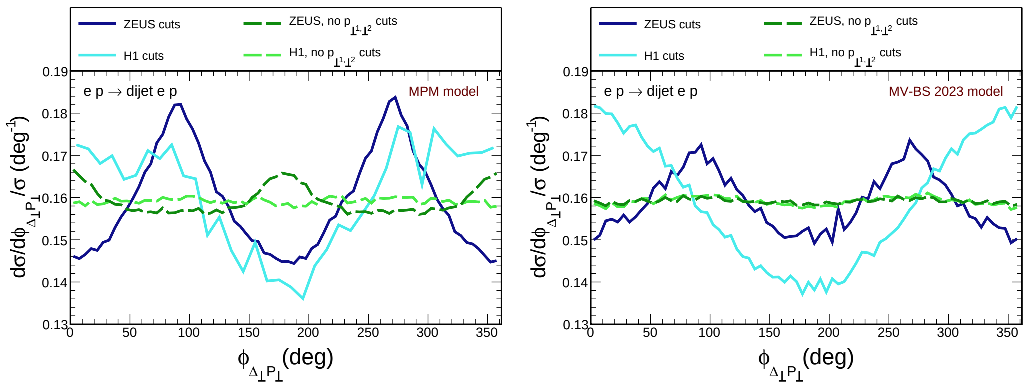

Figure 4: Distribution of the cross-section for the diffractive light dijet production in the energy of the photon-proton system (left) and azimuthal angle ϕ between $\vec{P}_\perp$ and $\vec{\Delta}_\perp$ (right) for H1 and ZEUS kinematic for different GTMDs. Notice the normalization.

distribution of the azimuthal angle between the sum and difference of the transverse jets' momenta. We predict that the straight horizontal line corresponds to the case without cuts on the transverse momentum of the jets, while the angular correlations can be seen for the situation in which cuts are included. We do not exclude the possibility that the additional azimuthal correlation may be due to elliptical gluon distributions, which were not taken into account in the presented analysis.

3. Conclusions

We discussed dijet correlations in the $ep \to epjj$ process. The corresponding differential distributions were calculated using various gluon GTMD (generalized transverse momentum dependent gluon distributions) distributions from the literature. We here calculated the distributions in various kinematic variables by referring to H1 and ZEUS data. The MV-BS, MPM, and MV-IR GTMD distributions describe some of the observables well but do not describe the distributions in $x_{\mathbb{P}}$ and β. Some of the other GTMD distributions are consistent with the H1 and ZEUS data. The most realistic gluon distributions seem to be GTMD KT and GBW, which give an insignificant contribution for H1, as it should be, and give a sizable contribution at $\beta > 0.5$ for the ZEUS cuts. This means that the considered mechanism is not sufficient.

We have also calculated correlations in azimuthal angles between the sum and difference of the transverse jets momenta. Since our GTMDs do not have an elliptical part, these correlations are solely the result of experimental cuts.

References

[1] F. Aaron *et al.*, The European Physical Journal C **72**, 1970 (2012).

[2] H. Abramowicz *et al.*, The European Physical Journal C **76**, 16 (2016).

[3] R. Pasechnik and M. Taševský, (2023), arXiv:2310.10793 [hep-ph].

[4] N. N. Nikolaev and B. G. Zakharov, Phys. Lett. B **332**, 177 (1994).

[5] N. N. Nikolaev, W. Schäfer, and G. Schwiete, Phys. Rev. D **63**, 014020 (2001).

[6] V. M. Braun and D. Y. Ivanov, Phys. Rev. D **72**, 034016 (2005), arXiv:hep-ph/0505263.

[7] B. Linek, A. Luszczak, M. Luszczak, R. Pasechnik, W. Schäfer, and A. Szczurek, JHEP **10**, 179 (2023).

[8] R. Boussarie, A. V. Grabovsky, L. Szymanowski, and S. Wallon, Phys. Rev. D **100**, 074020 (2019).

[9] Y. Hagiwara, Y. Hatta, and T. Ueda, Phys. Rev. D **94**, 094036 (2016).

[10] Y. Hagiwara, Y. Hatta, R. Pasechnik, M. Tasevsky, and O. Teryaev, Phys. Rev. D **96**, 034009 (2017).

[11] M. Reinke Pelicer, E. Gräve De Oliveira, and R. Pasechnik, Phys. Rev. D **99**, 034016 (2019).

[12] D. Boer and C. Setyadi, Phys. Rev. D **104**, 074006 (2021).

[13] D. Boer and C. Setyadi, Eur. Phys. J. C **83**, 890 (2023).

[14] K. J. Golec-Biernat and M. Wüsthoff, Phys. Rev. D 59, 014017 (1998).

[15] L. S. Moriggi, G. M. Peccini, and M. V. T. Machado, Phys. Rev. D **102**, 034016 (2020).

[16] H. Kowalski and D. Teaney, Phys. Rev. D **68**, 114005 (2003).

[17] L. D. McLerran and R. Venugopalan, Phys. Rev. D **49**, 3352 (1994).

[18] E. Iancu and A. H. Rezaeian, Phys. Rev. D **95**, 094003 (2017).

[19] M. Łuszczak, R. Maciuła, and A. Szczurek, Phys. Rev. D **91**, 054024 (2015).